EnvironmentAsia
The international journal by the Thai Society of Higher Education Institutes on Environment

EnvironmentAsia 18(1) 2025 110-125
DOI 10.14456/ea.2025.9
ISSN 1906-1714; ONLINE ISSN: 2586-8861

Synthesis of TiO_2 - Chitosan Nanocomposites-Based Antimicrobial Packaging and Its Application for Meat Product

Foliatini[1], Henny Rochaeni[2], Singgih Wibowo[1], Fachrurrazie[2], Suhartini[2*], and Putri Alfiani[1]

[1]Food Nanotechnology Department, Polytechnic of AKA Bogor, Jl. Pangeran Asogiri No. 283, Bogor 16154, Indonesia
[2]Chemical Analysis Department, Polytechnic of AKA Bogor, Jl. Pangeran Asogiri No. 283, Bogor 16154, Indonesia

*Corresponding author: suhartinijournal@gmail.com; suhartini@aka.ac.id
Received: September 3, 2024; Revised: October 25, 2024; Accepted: November 22, 2024

Abstract

Food packaging characteristics are highly important since their function is not only to package food but also to protect food from external materials such as oxygen and prevent mechanical disturbance, thus maintaining the food quality. Smart packaging, which also plays a role as active packaging, has the capability of inhibiting the growth of microorganisms, leading to a longer shelf-life of food. In this research, TiO_2/chitosan nanocomposite-based packaging was used since both TiO_2 and chitosan were proven as antimicrobial substances. Synthesis of the nanocomposite was conducted with the aid of ultrasonic energy to achieve higher efficiency. The results showed that the mechanical properties such as percentage of elongation, tensile strength, and young modulus of TiO_2/chitosan nanocomposite films meet the JIS standard. These films also have higher antimicrobial activity toward Bacillus and *Escherichia coli* compared to the amoxicillin standard. The thermal properties of the packaging films revealed that these films have sufficient thermal stability for application in the moderate range of temperatures. In addition, these films do not require high temperatures to decompose therefore they can decompose naturally in the environment as indicated by the results of biodegradability tests, which show a packaging degradation capacity of 7.43×10^{-4} g/day. The composition of the nanocomposite TiO_2/chitosan greatly affects the mechanical and antibacterial properties of the films.

Keywords: Nano-TiO_2; Ultrasonic energy; Nanochitosan; Nanocomposite; Active packaging; Antimicrobial activity; Mechanical properties

1. Introduction

Food packaging serves to maintain the quality of packaged food products during the process of storage, transportation, and consumption by consumers. The quality of food products in this case includes taste, appearance, and the nutrients they contain. Packaging must be able to protect food products from various deteriorative effects or damage caused by the external environment, such as microorganisms, as well as physical and chemical processes during distribution (Schaefer and Cheung, 2018). Thus, packaging has a major contribution to make in extending the shelf life and maintaining the quality and safety of food products. The quality of packaged food products is closely related to the characteristics of the food product and the packaging material used. Most food products will deteriorate due to mass transfer phenomena such as moisture absorption, oxygen ingress, flavor evaporation, unwanted odor absorption, and migration of packaging components into the food product. These phenomena can occur between the food

product and the atmospheric environment, between the food product and the packaging material, or between the various types of ingredients that are components in the food product (Alamri *et al.,* 2021). Food spoilage can also be caused by the contamination of various types of pathogenic bacteria and other microorganisms. Some types of microorganisms that often grow on food surfaces are Campylobacter, Salmonella, *Yersinia enterocolitica*, *Escherichia coli*, and *Listeria monocytogenes* (Huang *et al.,* 2019).

Research on creating antimicrobial packaging has been done to prevent damage from bacteria. The development of materials for antimicrobial packaging has been carried out either using commercial synthetic polymer films such as polyethylene-based polymers (Rokbani *et al.,* 2019), bio-based polymer films (Tan *et al.,* 2021), or polymer films that have natural antimicrobial characteristics, such as chitosan (Xing *et al.,* 2016). Chitosan is a biopolymer resulting from the deacetylation of chitin, which is generally extracted from arthropod animals (shrimp, lobsters, crabs, scorpions, and shellfish) (Azmana *et al.,* 2021). Chitosan is biocompatible, biodegradable, non-toxic, easy to modify, and can be broken down in the body (Biswal and Swain, 2023), therefore it is widely applied in various fields such as food, pharmaceuticals, cosmetics, health biotechnology, and the chemical industry. The high abundance of chitosan, its ability as an antimicrobial, and its ease of film formation (Wang *et al.,* 2017) make chitosan a potential raw material for food packaging.

Various studies have been conducted to produce food-active food packaging that has antimicrobial properties, including packaging in the form of citral and cinnamaldehyde stabilized by zein coupled with chitosan that can inhibit the activity of *Aspergillus westerdijkiae* in vitro and applied in food storage (Wang *et al.,* 2023). Another study was conducted by Wu *et al.* (2022), who studied the antifungal mechanism of essential oil against foodborne fungi in baked food. Various techniques to make antimicrobial packaging have been carried out, among others, by adding enzymes (Sharma *et al.,* 2022) and antimicrobials derived from essential oils of various types of plants (Varghese *et al.,* 2020), for example from thyme (*Thymus vulgaris*) (Talon *et al.,* 2016), lemon (Song *et al.,* 2017), garlic, and onion (Somrani *et al.,* 2020). Foods and drinks can vary greatly in their acidity or basicity, and adding enzymes has the drawback of having low-temperature stability and being readily influenced by pH. The addition of natural antimicrobials to food packaging is quite effective in increasing the stability of packaged food products.

Another alternative in designing antimicrobials is to use TiO_2, which has photocatalytic properties. Research on TiO_2-based antimicrobial packaging has been widely carried out, including by Kumaravel (Kumaravel *et al.,* 2021), who studied TiO_2 antimicrobial nanocomposite capabilities for orthopedic and dental surfaces. Although several studies regarding the negative impact of using TiO_2 in animals show genetic damage, inflammation, and the risk of tumor formation (Bischoff *et al.,* 2021), its application to humans requires paying attention to the gastrointestinal effects of TiO_2 on the lymphoid system and mucosa in the human intestine (Winkler *et al.,* 2018). The human body's interaction with TiO_2 nanoparticles is a complex system because of the biocompatibility of this metal oxide with various nutrients found in the body, such as glucose, age of the research object, molecular shape, particle size, dose, and exposure time (Chen *et al.,* 2020). The use of TiO_2 in food requires paying attention to the tolerance limit for the amount of TiO_2 that can be accepted by the human body. In the United States of America and India, the use of TiO_2 in food additives, for example as a bleach, must not exceed 1% (Brinas *et al.,* 2024). Several studies regarding the application of TiO_2 as an additional packaging material have been carried out. Research on the use of metal oxides in the form of TiO_2 nanoparticles in food packaging has been carried out to improve the physical, chemical, and antimicrobial properties (Zang and Rhim, 2022), as well as the ability to inhibit the photocatalytic activity of TiO_2, which can reduce contamination of food products and vegetable industry processing waste and fruit, and drinks to minimize the production

of ethylene gas in the ripening process so that TiO_2 can be used in active packaging (Berardinelli and Parisi, 2021). Riahi (Riahi *et al.,* 2020) have studied the effect of adding TiO_2 to gelatin with pomelo extract, which can prevent the transmission of UV rays so that it has antibacterial and antioxidant activity against *E. coli* and *L. monocytogenes*. It causes the addition of TiO_2 in the mixture to have the potential to be used in active packaging applications.

The development of nanotechnology has also produced a new material that has the potential to improve the stability of food products. The change in particle size to the nanoscale causes significant changes in properties, including surface area, reactivity, catalysis ability, texture, solubility, stability, absorption, and bioavailability (Joudeh and Linke, 2022). The size reduction of chitosan into nanochitosan can lead to changes in physicochemical properties, such as a larger surface area resulting in more cationic groups and higher reactivity. This has the potential to increase the charge interaction on the surface, which can improve the antibacterial ability (Grala *et al.,* 2021).

Particle size and chitosan concentration have significant effects on the film's antibacterial performance. Nanochitosan has a greater number of charged amino groups, which can increase interactions with negatively charged bacterial cells so that its antimicrobial properties increase (Jhaveri *et al.,* 2021). The utilization of nanochitosan as a film has been studied by Shahbazi and Shavisi (2018), who showed that nanochitosan films that have been added with Mentha spicata essential oil and methanolic extracts of pomegranate peel and grape seeds have antibacterial and antioxidant activities that can prevent chemical and microbial contamination in the food industry. Cellulose films with antimicrobial capabilities have also been successfully prepared by adding nanochitosan.

Based on the above problems, authors are very interested in developing smart, biodegradable packaging, especially for meat products. Active packaging technology on this biodegradable plastic packaging has advantages in terms of its antimicrobial properties due to chitosan and TiO_2 nanocomposites. This study aimed to synthesize TiO_2/chitosan nanocomposite films and apply them as antimicrobial packaging for meat products. The addition of TiO_2 nanoparticles has been proven to improve the physical properties, thermal stability, mechanical properties, chemical properties, and antimicrobial properties of packaging and can extend the shelf life of food (Sani *et al.,* 2022). Using this nanocomposite can improve the texture, thermal, mechanical, optical, gas barrier, antimicrobial, and biodegradability of packaging so that it is environmentally friendly (Anaya-Esparza *et al.,* 2020). This combination of biodegradable material and antimicrobial properties is expected to be very beneficial for all parties, especially in reducing food and packaging waste, preventing product spoilage before consumption, protecting the product from external causes of deteriority, maintaining the quality of the product, and resulting in a longer shelf-life of the product.

2. Methodology

2.1 Materials

The materials used consisted of chitosan obtained from household production in Bogor, West Java, acetic acid (Merck), titanium dioxide (Merck), gelatin (HAYS Food), glycerin (Merck), *E. coli., Bacillus sp.,* fresh meat, Mullen Hinton Agar (MHA), disc paper, sodium chloride (Merck), and aquadest. The equipment used consisted of Dry Herbs Grinding Milling Type C2100Y, Test Sieve Shaker Type Haver ELM 200 Premium, Universal Testing Machines Type X350-5, Spectrophotometer Fourier Transform Infrared (FTIR) Alpha Bruker, Spectrophotometer UV-Vis Type Specord 200 Plus, ultrasound-assisted extraction (UAE), differential scanning calorimetry, oven (LabTech), silicone mold, analytical balance type ATX224 (LabTech), magnetic stirrer, silicone mold, and glassware (pyrex).

2.2 Synthesis of nanochitosan

The preparation of chitosan nanoparticles was carried out using the ultrasound-assisted extraction (UAE) method in stages: chitosan

was pulverized using dry herbs grinding milling and sieved with a test sieve shaker until a 325 mesh size was obtained. Chitosan was weighed and dissolved in 100 mL of 1% CH3COOH, with mass variations of 0.5, 0.75 and 1 g. The mixture was stirred for an hour. Each mixture was stirred for 1 hour at 80oC at 1000 rpm until dissolved. The solution obtained was sonicated for 2 hours at 50% amplitude. The chitosan solution formed was characterized using a particle size analyzer (PSA) to determine the particle size formed. Nanochitosan was obtained from food packaging with TiO_2 composites using gelatin and glycerin as plasticizers.

2.3 Synthesis of a nano-TiO_2 solution

A total of 20 mg of TiO_2 was mixed into 400 mL of acetic acid and then sonicated for 2 hours with 50% amplitude. A total of 10 g of gelatin and 2.5 g of food-grade glycerol were dissolved in 400 mL of a sonicated TiO_2 solution.

2.4 Synthesis of active packaging

A combination of nanochitosan and nano-TiO_2 solution was used to create bioplastics; the ratio of nanochitosan to nano-TiO_2 was varied. The mixture was homogenized using a hotplate magnetic stirrer for several minutes. The mixture was placed onto a petri dish and was done in an oven at 55 °C for 24 hours.

2.5 Characterization of nanochitosan and TiO_2 /chitosan nanocomposite film

The determination of particle size and size distribution was carried out using a particle size analyzer (PSA). Functional group analysis was carried out to determine the interactions that occur between components in smart packaging using the Alpha Bruker Fourier Transform Infrared (FTIR) Spectrophotometer at a wavelength of 400 - 4000 cm^{-1} (Shahbazi and Shavisi, 2018). Mechanical properties tests were carried out using Universal Testing Machines Type X350-5 to determine tensile strength, Young's modulus, elongation at break (EAB), and thickness. Measurements refer to ASTM D-882-10 (ASTM D-882, 2017).

The Smart Packaging Transparency Test was carried out using a UV-Vis spectrophotometer at a wavelength of 600 nm (Binsi *et al.,* 2013). The darkness index is calculated by the equation:

$$\text{darkness index} = \frac{\text{Abs}_{600}}{\text{X}}$$

Abs_{600} is absorption at a wavelength of 600 nm, and X is Smart Packaging thickness.

The water absorption test refers to ASTM D570-98 (ASTM D570-98, 2010), which is carried out by printing Smart Packaging with a diameter of 5 cm and a maximum thickness of 0.32 cm, drying it, and weighing it initially. Smart Packaging is completely immersed in a container containing distilled water at a temperature of 23 ± 1°C for 24 hours, removed from the container, dried with filter paper, and weighed finally. The following formula is used to get the darkness index:

$$\text{Water absorption (\%)} = \frac{w_1 - w_0}{w_0} \text{ x } 100$$

W_1 is the mass of water after immersion and w_0 is the mass of water before immersion.

2.6 Antimicrobial analysis of TiO_2 /chitosan nanocomposite film

Antimicrobial analysis used the disc diffusion method, which was carried out by dissolving 19 g of Mullen Hinton Agar (MHA) with 500 mL of distilled water, sterilizing it at 121 °C for 15 minutes with an autoclave, then 25 mL of the solution was poured into a petri dish until it solidified. The amount of 1 mL of *E. coli* and *Bacillus sp.* suspension in physiological NaCl solution was inoculated into MHA media, spread evenly with a hockey stick, and left to dry. On the surface of the media, a disc paper that has been soaked in Smart Packaging suspension is placed aseptically. The clear zone around the paper disc was measured at different positions, and the values were averaged. The results obtained were compared with amoxicillin as a standard.

2.7 Application of TiO_2/chitosan nanocomposite film as meat packaging

The TiO_2/chitosan nanocomposite packaging film that has been made is then applied to package meat by wrapping the meat from the day of purchase until it rots at room temperature. Color and odor observations were made every 24 hours.

2.8 Biodegradability test of TiO_2/chitosan nanocomposite film

The Smart Packaging biodegradability test was carried out using the soil burial method (Tharoke *et al.,* 2001), accompanied by several modifications by means of Smart Packaging measuring 5 x 5 cm being buried in compost soil at a depth of 4 cm. The soil is watered periodically (once a day) for 15 days. Smart Packaging was removed, rinsed with distilled water, and dried in the oven until constant weight. The smart packaging degradation rate is calculated using the relationship between sample weight loss and time.

3. Results and discussion

3.1 Synthesis of nanochitosan

Chitosan nanoparticles have been successfully synthesized via a simple and greener route using ultrasonic energy. This type of energy has a high frequency (> 20 kHz), thus it has the capability of breaking chemical bonds and micro-aggregates by vibration as an energy source (Khoerunnisa *et al.,* 2021). The excellent properties of ultrasonic energy made it applicable in chemical synthesis, including bottom-up-based nanochitosan preparation (Boufi *et al.,* 2017).

The selection of the synthesis method for nanoparticles is commonly based on some considerations, including efficiency. High-efficiency methods lead to a higher abundance of nanoparticles in a short reaction time. High temperature and pressure bubbles cause cavitation events in ultrasonic-based processes, which encourage precursor molecules to collide more frequently and, as a result, yield a higher amount of synthesis (Ferodov *et al.,* 2022). Besides reaction using ultrasonic energy, another method commonly used by researchers to synthesize nanochitosan is ionic gelation; however, this method involves chemicals and thus does not match the demand for green synthesis. Moreover, the synthesis of nanochitosan by ionic gelation requires a longer time, and there is difficulty in obtaining high monodispersity in particle size (Hoang *et al.,* 2022).

The characterization of nanochitosan by the particle size analyzer revealed that the concentration of chitosan in the precursor solution influences the particle size and distribution of nanochitosan. The higher the concentration of chitosan solution, the larger the particle size of nanochitosan. Moreover, the particle size distribution at higher concentrations was broader, as shown by the polydispersity index (Table 1). At a concentration of 1% chitosan solution, the particle size was larger than 1 μm. When the chitosan concentration was reduced to 0.75%, particles with a size in the nanometer range were formed, at an average of 397 nm. In this condition, large particles above 1 μm were still found, but with a relatively low volume. The volume value of 92.9% for particles having a size of 397 nm indicates that most of the as-synthesized chitosan nanoparticles have an average size of 397 nm. As the chitosan concentration got lower to 0.5%, smaller

Table 1. Effect of chitosan concentration on particle size

Sample	Chitosan (%)	Particle Size (nm)	Volume (%)	Polydispersity Index (PDI)
1	0.50	376	87.5	0.2658
		189.1	12.5	
2	0.75	1865	7.1	0.321
		397	92.9	
3	1.00	1084	100	0.461

particles formed with averages of 376 nm and 189.1 nm. In this condition, the result of the PSA analysis revealed two peaks of average particle size with a large difference in volume, which means that particle size was not homogeneous. Assuming that the growth of particles follows a coalescence mechanism, the higher concentration of precursor molecules is related to the higher probability of the combination of molecules forming larger particles. The % volume of 87.5% and 12.5% of each kind of particle size showed that at a chitosan concentration of 0.5%, the growth could not be controlled, leading to an intense agglomeration. However, at a chitosan concentration of 0.75%, most particles have almost the same size, as shown by the large volume. This result indicated that the optimum chitosan concentration for achieving monodispersed nanoparticles was 0.75%.

El-Naggar *et al.* (2022) have studied the effect of several variables, including initial pH, incubation time, chitosan concentration, and temperature, on nanochitosan biosynthesis using the Box-Behnken design. From variance analysis using ANOVA, the P-value that is lower than 0.05 indicates that the coefficient of these above variables is significant and could be a limiting factor that influences the rate of nanochitosan biosynthesis. Positive values of the coefficient for chitosan concentration showed a linear interaction between the increment of chitosan concentration and the rate of nanochitosan biosynthesis. The synthesis rate may significantly affect the particle size, shape, and distribution. The conclusion of the previous research was in agreement with the result of this study.

Several studies have been performed to explain the nanochitosan synthesis and report the range of particle size. Some of them succeeded in obtaining sizes below 100 nm and others above 100 nm, depending on the experimental methods and conditions. Khanmohammadi *et al.* (2015) found that the as-prepared nanochitosan has an average particle size in the range of 33.64 nm to 74.87 nm. Abdullah *et al.* (2022) have succeeded in making spherical chitosan nanoparticles with a size of 50 ± 5 nm.

3.2 Preparation of active packaging

The as-prepared nanochitosan is combined with TiO_2 in several compositions, as listed in Table 1. To increase the solubility and dispersibility of TiO_2 in the mixture, ultrasonication of the TiO_2 solution was performed before mixing with nanochitosan and gelatin. This step resulted in a clear, yellowish solution without any precipitation (Figure 1). After being poured into the silicon mold and treated at a moderate temperature for some hours, transparent films were obtained and then subjected to mechanical, thermal, and chemical analysis.

3.3 Characterisation of Active Packaging

3.3.1 Mechanical Properties

Using a Universal Testing Machine (UTM), the mechanical characteristics of

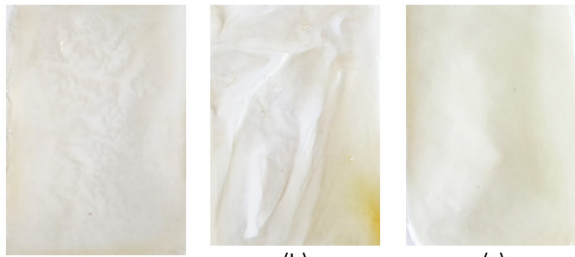

(a) nanochitosan:GGT (1:3),
(b) nanochitosan:GGT (1:1),
(c) nanochitosan:GGT (3:1) with GGT is gelatin-gliserol-TiO_2

Figure 1. Appearance of the packaging film

TiO_2/chitosan-based nanocomposite films were examined. The nanochitosan films, in the absence of TiO_2 were also evaluated for comparison. The result showed that at chitosan concentrations of 0.5% and 0.75%, the film thickness was similar; however, at higher concentrations (1.0%), the thickness was slightly increased. The resulting film thickness data meets the requirements when using the JIS standard reference, which is < 0.25 m (Table 3). The amount of data collected is less than that of earlier studies by Kumar *et al.* (2021). The study reported that the thickness of chitosan films modified with pomegranate peel extract was in the range of 0.142 ± 0.05 mm to 0.159 ± 0.04 mm.

In addition to thickness, the film was also tested with a Universal Testing Machine (UTM) to evaluate its mechanical properties. One of the mechanical properties tested was elongation. Based on Table 2, the percent elongation of the three film variations is significantly different. The increase in chitosan concentration to 0.75% increased percent elongation, but at 1% concentration, the percent elongation decreased, although the value obtained was still higher than at 0.5% chitosan concentration. The percent elongation values of the three chitosan concentration variations still meet the requirements of edible films according to JIS standards and are still classified as good percent elongation values because they are > 50%.

Another variable tested was Young's modulus, which is a parameter that indicates the ease of strain and deformation. Young's modulus is the ratio of tensile strength to tensile strain. If the tensile strength is much greater than the tensile strain, the film tends to be stronger, stiffer, and less elastic. The tensile strength value has been met for the concentration variations of 0.75% and 1%, while for the chitosan concentration of 0.5%, the value is still slightly below the JIS standard.

3.3.2 Fourier Transform Infrared (FT-IR) Spectroscopy Analysis

The packaging films obtained were tested using FTIR spectroscopy to evaluate the changes in functional groups that occur during mixing and film formation. Although analysis using FTIR spectroscopy cannot determine the structure in detail, it is very useful for predicting structural changes that occur during the process, which can be seen from the shift in wave numbers, the increase or decrease in transmittance peaks, and the formation of new peaks.

Figure 2 shows that the spectrum of the initial chitosan has several peaks, including those at wave numbers 1571 cm^{-1} and 1651 cm^{-1}, which are N-H bending in primary amines and C = O stretching vibrations in amides, respectively. The peaks between wave numbers 995 cm^{-1} and 1090 cm^{-1} are -C-O-H and -C-O-C stretching vibrations. These peaks look jagged because they are composed of several small peaks with adjacent wave numbers, which indicate groups with a variety of different chemical environments.

Table 2. UTM test result data for samples with variations in chitosan concentration of 0.5 - 1.0%

Concentration of chitosan (%)	Thickness (mm)	Elongation at peak (mm)	E (%)	Force at peak (N)	Stress at peak (N/mm^2)	Strain at peak (%)	Strain at break (%)	Young modulus (N/mm^2)
0.5	0.07	6.362	63.63	2.66	3.8	6.362	6.797	97.171
0.75	0.07	11.729	117.29	12.41	17.729	11.723	11.897	673.497
1.0	0.1	7.161	71.61	21.65	21.65	7.161	7.376	2150.845

Table 3. Edible film standards according to JIS

Characteristics of edible films	Edible film standards according to JIS
Thickness (mm)	< 0.25
Tensile strength (MPa)	> 3.92266
Elongation (%)	Bad < 10% Good > 50%
Young modulus (MPa)	> 0.35
WVTR ($g/m^2.h$)	< 10

Peaks in this area are often used to prove that the chitosan structure is formed through glycosidic bonds (Rochima *et al.,* 2017). The peak at wave number 1149 cm^{-1} indicates the stretching vibration of CN bound to NH_2, which is evidence of the formation of amine groups. The peak at wave number 1425 cm^{-1} indicates stretching vibrations of C-N (amide) bonds, while the peak at 1378 cm^{-1} is an indication of the presence of acetyl groups. The stretching vibrations of -OH and -NH and the interaction between molecules in the form of hydrogen bonds are seen from the peaks in the range of 3000 - 3600 cm^{-1}. As is common with other organic compounds, the FTIR spectrum also shows peaks at 2800 - 2900 cm^{-1} indicating the presence of methyl and methylene groups in the chitosan structure.

The FTIR spectrum of nanochitosan, or chitosan that has undergone ultrasonication, does not undergo significant changes when compared to the initial chitosan. After ultrasonication, the peak of the OH group in the region around 3000-3600 cm^{-1} is slightly reduced in intensity, and the peak at 1615 cm^{-1} shifts to the right to 1577 cm^{-1}. By mixing with gelatin in glycerol, slight changes occurred; among others, the intensity of the peak for the -OH group is greater due to the additional -OH groups from gelatin and glycerol The presence of OH groups in gelatin-glycerol can be observed by a strong peak in the 3000 -3600 cm^{-1} area. The second change occurs in the 1590 - 1660 cm^{-1} region, which increases significantly.

The FTIR spectrum of TiO_2 shows a sharp peak at wave numbers 1461 cm^{-1} and 1023 cm^{-1}. The peak at 1023 cm^{-1} indicates the presence of Ti-OH bonds. The peak at 600 - 900 cm^{-1} shows the Ti-O asymmetric stretching mode. Ti-O-Ti stretching vibrations in the region around 400 - 500 cm^{-1} (Spoială *et al.,* 2022) are not visible in the spectrum because the measurements were made in the range of 650 - 4000 cm^{-1}.

In this study, it was found that there was a slight shift in wave number from 3301 cm^{-1} in nanocitosan to 3285 cm^{-1} in TiO_2/Chitosan nanocomposite. Spoială (Spoială *et al.,* 2022) reported that the presence of TiO_2 bound to chitosan can cause peak shifts, especially in the -OH, -NH, and stretching C = O amide functional group regions. This implies the creation of contacts between TiO_2 and chitosan via the groups. The decrease in the wave number value obtained in this study indicates that there is an interaction between the -Ti-O bond and -OH or -NH from chitosan. This means that chitosan and TiO_2 are not only physically mixed but can also form strong intermolecular interactions between certain groups, for example, between -Ti-O groups or between -OH and -NH groups with -C-O-chitosan. Anaya-Esparza *et al.* (2020) explains the possible interactions between TiO_2 and chitosan as follows;

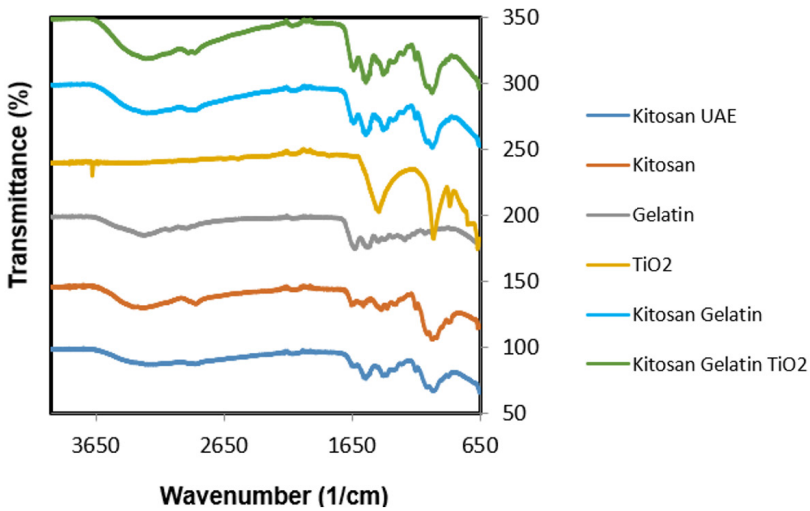

Figure 2. FTIR spectra for chitosan, nanochitosan synthesized by ultrasonication, gelatin, TiO_2, chitosan-gelatin, and chitosan-gelatin-TiO_2

3.3.4 Thermal Analysis

DSC analysis displays data on thermal properties, including melting point and enthalpy of melting. It is evident from the data in Table 4 and Figure 4 that the composition of the nano-TiO_2 and nanochitosan that make up the composite film affects the melting point of the TiO_2/chitosan nanocomposite film. The fairly low melting point allows the packaging film to be easily degraded. Table 1 shows samples 1 and up to 3, namely ratios 1:1 and 3:1.

The results obtained are similar to those of Acosta-Ferreira *et al*. (2020). Previous research shows that chitosan with a concentration of 1% - 3% has a melting point of around 135 °C to 169 °C with an enthalpy in the range of 77 J/g-122 J/g (Acosta-Ferreira *et al.,* 2020). Measurements of the thermal properties of chitosan/TiO_2 nanocomposite bioplastic film are shown in Figure 4.

3.3.5 Transparency Analysis

The transparency test results show that composition affects the opacity index. Increasing chitosan concentration results in an increase in the opacity index. This is due to more polymer chains blocking light transmission, making the film less transparent. Film transparency for packaging is related to aesthetics. For packaging in the form of a thin coating to cover meat or fruits, a highly transparent film is generally required. Previous studies reported that petroleum-based packaging presents transmittance values in the range of 85 – 90% and high-transparent polymers such as gelatin, chitosan, and poly (vinyl alcohol) (PVA) exhibit opacity values < 1. Transparent bio-based polymers such as calcium alginate, cellulose acetate, carboxymethyl cellulose, and carrageenan and petroleum-based polymers such as polystyrene, OPP, and LDPE have opacity values in the range of 1 - 5. Thus, the result obtained in this study was in agreement with the previous study.

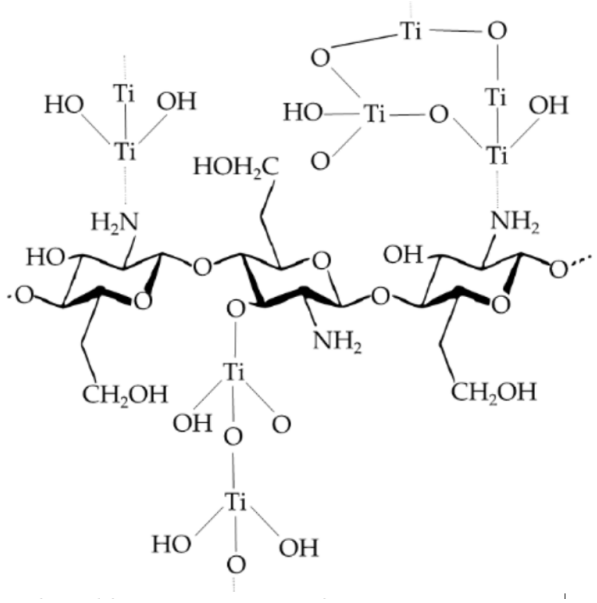

Figure 3. TiO_2-chitosan nanocomposite structure (Anaya-Esparza *et al.,* 2020)

Table 4. Melting point and melting enthalpy for chitosan/TiO_2 nanocomposite

Sample	Melting point (°C)	ΔH melting (J/g)
1: 1	91.046	392.958
1: 3	133.249	238.567
3: 1	91.173	341.536

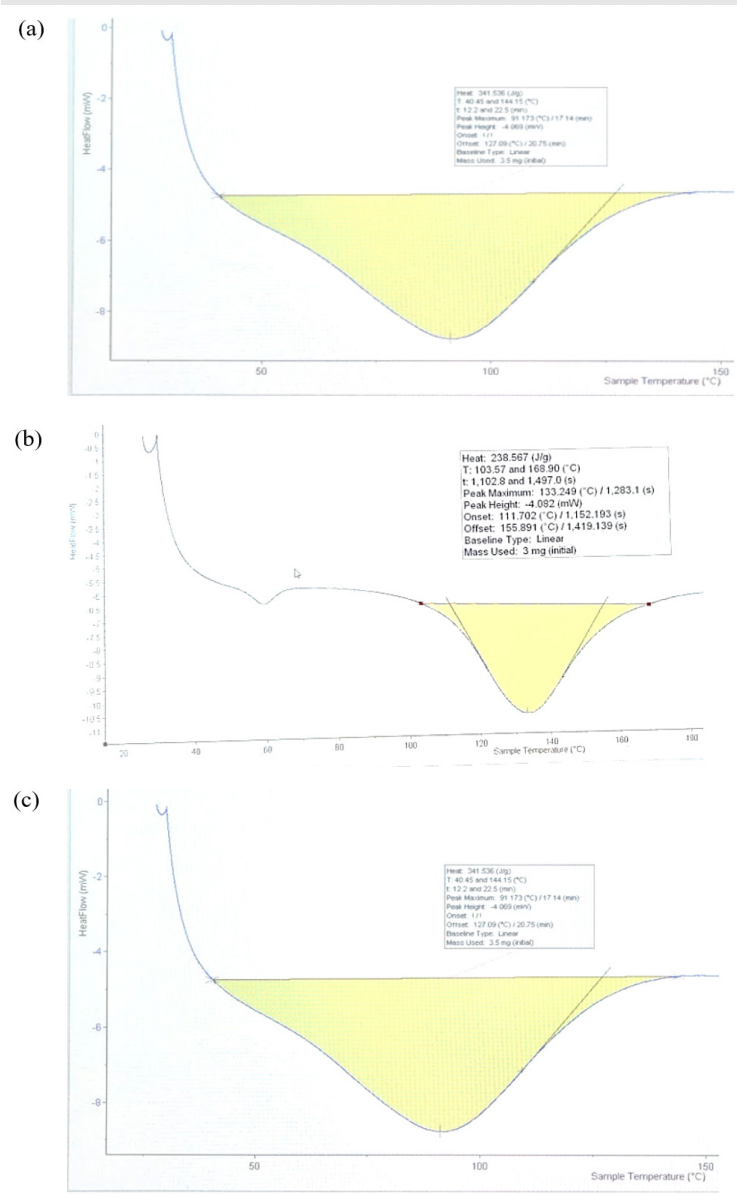

(a) 1:1, (b) 1:3, (c) 3:1

Figure 4. Thermogram curve from DSC for chitosan/TiO_2 nanocomposite, at various ratios

Table 5. Darkness index for nanochitosan and nanochitosan/TiO_2

Material	Absorbance at 600 nm	Film thickness (mm)	Darkness index
Chitosan 0.5%	0.0604	0.07	0.863
Chitosan 0.75%	0.0786	0.07	1.123
Chitosan 1.0%	0.1425	0.1	1.425
Chitosan: GGT (1:1)	0.0629	0.083	0.758
Chitosan: GGT (1:3)	0.1725	0.07	2.464
Chitosan: GGT (3:1)	0.1038	0.057	1.821

3.3.6 Antimicrobial Analysis

Inhibition test results using the agar diffusion method showed that TiO_2 in the absence of chitosan had higher antimicrobial activity against *E. coli*, but lower activity against *Bacillus sp*. compared to the standard amoxicillin. Bare chitosan without TiO_2 can have better antimicrobial activity than TiO_2, but it can also be lower depending on the concentration. At a relatively low concentration of 0.5%, antimicrobial activity against *E. coli* was high but had no antimicrobial activity against Bacillus. Chitosan at 0.75% concentration had lower antimicrobial activity against *E. coli* but higher activity against *Bacillus sp*. At an even higher concentration of 1%, the inhibition against both *E. coli* and *Bacillus sp*. was higher than the standard. At this concentration, the inhibition against *Bacillus sp*. was almost the same compared to the 0.75% concentration and almost the same as the inhibition against *E. coli* compared to 0.5% chitosan.

In the nanocomposites, it was clear that the combination of two materials with antimicrobial potential resulted in significantly greater inhibition against *E. coli* but relatively no effect on the inhibition against *Bacillus sp*., even for chitosan: a GGT ratio of 3:1, the inhibition against *Bacillus sp*. was smaller than the standard. For inhibition against *E. coli*, the most optimum chitosan-TiO_2 combination is 1:3 because it produces the highest inhibition, i.e., 1.4 cm, or 75% higher than that of the standard.

3.4 Application of Nanocomposite Film as Meat Packaging

Based on antimicrobial analysis, the TiO_2/chitosan nanocomposite film composition with a chitosan and GGT ratio of 1:3 was applied as meat packaging because it has greater inhibitory power against *E. coli* and *Bacillus sp*. when compared with amoxicillin. The chitosan/TiO_2 nanocomposite packaging film that has been made is then applied to package meat, as shown in Figure 5. Storage is carried out at room temperature from purchase until the meat rots.

The results obtained showed that the chitosan/TiO_2 nanocomposite packaging film was only slightly better at maintaining the quality of the packaged meat. Green stains and an overpowering stench indicated that the meat in the traditional packaging had begun to decay by the second day. In meat packaged with chitosan/TiO_2 nanocomposite, storage until the second day still showed the characteristics of relatively fresh meat, even though there was a slight change in color to a

Table 6. The inhibitory power of chitosan/TiO2 nanocomposites against *E. coli* and *Bacillus sp*.

Material	Inhibitory power (cm)	
	E. coli	*Bacillus sp.*
Standard	H = 0.8	H = 1.0
	V= 0.8	V= 1.0
TiO_2	H = 0.9	H = 0.8
	V= 0.9	V= 0.8
Chitosan 0.5%	H = 1.4	H = 0.0
	V= 1.1	V= 0.0
Chitosan 0.75%	H = 0.6	H = 1.4
	V= 0.6	V= 1.3
Chitosan 1.0%	H = 0.9	H = 1.4
	V= 0.9	V= 1.1
Chitosan: GGT (1:1)	H = 1.2	H = 1.0
	V= 1.1	V= 1.1
Chitosan: GGT (1:3)	H = 1.4	H = 1.1
	V= 1.4	V= 1.1
Chitosan: GGT (3:1)	H = 1.0	H = 0.8
	V= 1.3	V= 0.8

H=horizontal, V=vertical, nanochitosan 0.75%

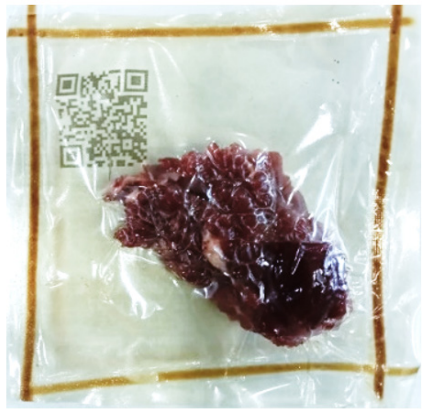

Figure 5. Beef packaging uses chitosan/TiO_2 nanocomposite film

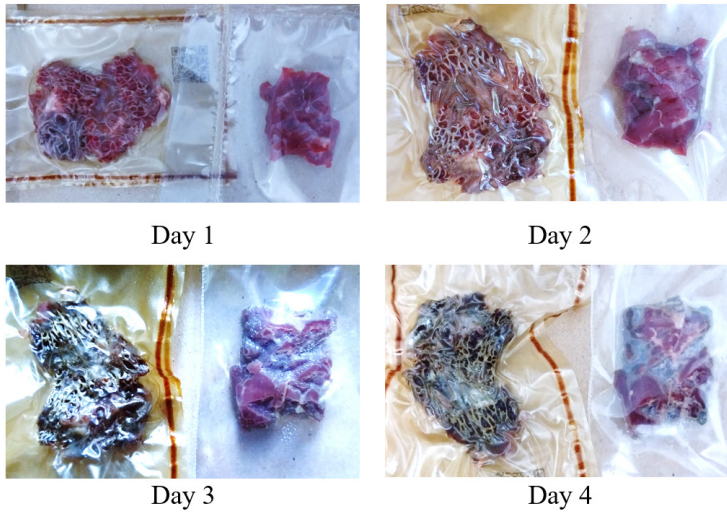

Figure 6. Meat packaging uses chitosan/TiO_2 nanocomposite packaging film at varying times of 1 to 4 days

darker color. A significant change in properties occurred on the 4th day, namely that it started to produce a foul smell, so it can be concluded that on the 4th day, the meat was no longer suitable for consumption. The appearance of meat packaging for 4 days can be seen in Figure 6.

3.5 Biodegradability Tests of Nanocomposite Film as Meat Packaging

Biodegradability tests are carried out to determine the ability of packaging materials to degrade in the environment. The biodegradability test was carried out by planting packaging materials of known mass in the soil for 14 days. The degradation rate of packaging materials is calculated using the relationship between sample weight loss and time, the results of which can be seen in Table 7.

Table 7 shows that sonication causes food ingredients to degrade more easily because physical degradation occurs due to the use of ultrasonic energy during the sonication process. In addition, the addition of the TiO_2 mixture significantly increases the biodegradability of packaging materials under optimum conditions at the nanochitosan:GGT ratio (1: 1). This is related to the high water absorption capacity, which reaches 80%, thereby accelerating the chemical degradation process in soil containing organic acids.

Table 7. Biodegradability test results of Nanocomposite Film as Meat Packaging

Packaging materials	Initial mass (g)	Final mass (g)	Degradation rate (g/day)
Chitosan without UAE	0.0116	0.0114	1.43×10^{-5}
Chitosan 0.5%	0.0229	0.0204	1.79×10^{-4}
Chitosan 0.75%	0.0149	0.0140	6.42×10^{-5}
Chitosan 1.0%	0.0263	0.0234	2.07×10^{-4}
Nanochitosan: GGT (1:1)	0.0312	0.0208	7.43×10^{-4}
Nanochitosan: GGT (1:3)	0.0545	0.0102	3.16×10^{-3}
Nanochitosan: GGT (3:1)	0.0306	0.0268	2.71×10^{-4}

4. Conclusion

In this research, antimicrobial packaging made from TiO_2-chitosan nanocomposites has been successfully synthesized using the UAE method. With a thickness of less than 0.25 mm (per JIS standards) and a melting enthalpy of 238.567 J/g, the maximum antibacterial efficacy was achieved at a ratio of 0.75% nanochitosan and nano-TiO_2 of 1:3. Antimicrobial packaging has better inhibitory power than amoxicillin against *E. coli* and *Bacillus sp*. and can extend the shelf life of meat for 4 days at room temperature.

Acknowledgment

Thanks to the Industrial Human Resources Development Agency (BPSDMI) of the Ministry of Industry and AKA Bogor Polytechnic for all the support and assistance provided so that this research can run well.

References

Abdullah AS, El Sayed IET, El-Torgoman AMA, Kalam A, Wageh S, Kamel MA. Green Synthesis of Silymarin–Chitosan Nanoparticles as a New Nano Formulation with Enhanced Anti-Fibrotic Effects against Liver Fibrosis. International Journal of Molecular Sciences 2022; 23 (10): 1-32.

Acosta-Ferreira S, Castillo OS, Madera-Santana JT, Mendosa-Garcia DA, Nũńez-Colĩn CA, Grijalva-Verdugo C, Villa-Lerma AG, Morales-Vargas T, Rodrĩguez- Nũńez JR. Production and physicochemical characterization of chitosan for the harvesting of wild microalgae consortia. Biotechnology Reports 2020; 28: e00554.

Alamri MS, Qasem AAA, Mohamed AA, Hussein S, Ibraheem MA, Shamlan G, Alqah HA, Qasha AS. Food packaging's materials: A food safety perspective. Saudi Journal of Biological Sciences 2021; 28(8): 4490–4499.

Anaya-Esparza LM, Ruvalcaba-Gómez JM, Maytorena-Verdugo CI, Gonzălez-Silva N, Romero-Toledo R, Aguilera-Aguirre S, Pĕrez-Larios A, Montalvo-Gonzălez E. Chitosan-tio2: A versatile hybrid composite. Materials 2020; 13 (4): 1-27.

ASTM International. Standard test methods for tensile properties of thin plastic sheeting, method D882-10. IHS, West Conshohocken, United States. 2017.

ASTM International. Standard Test Method for Water Absorption of Plastics. Pennsylvania (US). 2010.

Azmana M, Mahmood S, Hilles AR, Rahman A, Bin Arifin MA, and Ahmed S. A review on chitosan and chitosan-based bionanocomposites: Promising material for combatting global issues and its applications. International Journal of Biological Macromolecules 2021; 185 (June): 832–848.

Berardinelli A, Parisi F. 11-TiO_2 in food industry and cosmetics. Titanium Dioxide (TiO_2) and Its Applications 2021; 353-371.

Binsi PK, Ravishankar CN, Srinivasa Gopal TK. Development and Characterization of an Edible Composite Film Based on Chitosan and Virgin Coconut Oil with Improved Moisture Sorption Properties. Journal of Food Science 2013; 78 (4): 526-534.

Bischoff NS, de Kok TM, Sijm DTHM, van Breda SG, Briede JJ, Castenmiller JJM, Opperhuizen A, Chirino YL, Dirven H, Gott D, Houdeau E, Oomen AG, Poulsen M, Rogler G, van Loveren H. Possible adverse effects of food additive E171 (Titanium Dioxide) related to particle specific human toxicity, including the immune system. International Journal of Molecular Sciences 2021; 22 (207): 1-35.

Biswal A, Swain SK. Chitosan: A Smart Biomaterial. In: Swain SK, Biswal A (eds) Chitosan Nanocomposites. Biological and Medical Physics, Biomedical Engineering. Springer, Singapore. 2023.

Boufi S, Haaj SB, Magnin A, Pignon F, Impĕror-Clerc M, Mortha G. Ultrasonic assisted production of starch nanoparticles: Structural characterization and mechanism of disintegration. Ultrasonics Sonochemistry 2018; 41 (March): 327–336.

Brinas R, Dessipri E, Srinivasan JR, Walch S. Titanium dioxide. 97th JECFA-Chemical and Tecchnical Assessment (CTA) 2024 @FAO 2024.

Chen Z, Han S, Zhou S, Feng H, Liu Y, Jia G. Review of health safety aspects of titanium dioxide nanoparticles in food application. Nano Impact 2020; 18: 100224.

El-Naggar NEA, Shiha AM, Mahrous H, Mohammed ABA. Green synthesis of chitosan nanoparticles, optimization, characterization and antibacterial efficacy against multi drug resistant biofilm-forming Acinetobacter baumannii. Scientific Reports 2022; 12 (19869): 1–19.

Escárcega-Galaz AA, Sánchez-Machado DI, López-Cervantes J, Sanches-Silva A, Madera-Santana TJ, Paseiro-Losada L. Characterization data of chitosan-based films: Antimicrobial activity, thermal analysis, elementary composition, tensile strength and degree crystallinity. Data in Brief 2018; 21: 473–479.

Fedorov K, Dinesh K, Sun X, Soltani RDC, Wang Z, Sonawane S, Boczkaj G "Synergistic effects of hybrid advanced oxidation processes (AOPs) based on hydrodynamic cavitation phenomenon – A review. Chemical Engineering Journal 2022; 432 (134191).

Grala D, Biernacki K, Freire C, Kuźniarska-Biernacka I, Souza HKS, Gonçalves MP. Effect of natural deep eutectic solvent and chitosan nanoparticles on physicochemical properties of locust bean gum films. Food Hydrocolloids 2022; 126(107460).

Hoang NH, Thanh TL, Sangpueak R, Treekoon J, Saengchan C, Thepbandir W, Papathoti NK, Kamkaew A, Buensanteai N. Chitosan Nanoparticles-Based Ionic Gelation Method: A Promising Candidate for Plant Disease Management. Polymers 2022; 14 (4): 1–28.

Huang T, Qian Y, Wei J, Zhou C. Polymeric antimicrobial food packaging and its applications. Polymers 2019; 11 (3): 1-18.

Jhaveri J, Raichura Z, Khan T, Momin M, Omri A. Chitosan nanoparticles-insight into properties, functionalization and application in drug delivery and theranostics. Molecules 2021; 26 (272): 1-29.

Joudeh N, Linke D. Nanoparticle classification, physicochemical properties, characterization, and applications: a comprehensive review for biologists. Journal and Nanobiotechnology 2022; 20(1): 1–29.

Khoerunnisa F, Yolanda YD, Nurhayati M, Zahra F, Nasir M, Opaprakasit P, Choo M-Y, Ng N-P. Ultrasonic Synthesis of Nanochitosan and Its Size Effects on Turbidity Removal and Dealkalization in Wastewater Treatment. Intentionas 2021; 6 (4): 1–12.

Khanmohammadi M, Elmizadeh H, Ghasemi K. Investigation of Size and Morphology of Chitosan Nanoparticles Used in Drug Delivery System Employing Chemometric Technique. Iranian Journal of Pharmaceutical Research 2015; 14 (3): 665–675.

Kumaravel V, Nair KM, Mathew S, Bartlett J, Kennedy JE, Manning HG, Whelan BJ, Leyland NS, Pillai S. Antimicrobial TiO_2 nanocomposite coatings for surfaces, dental and orthopaedic implants. Chemical Engineering Journal 2021; 416(July): 1-19.

Kumar N, Patel M, Nguyen TT, Kim S, Kim J. Effect of TiO_2 layer thickness of TiO_2/NiO transparent photovoltaics. Progress in Photovoltaics: Research and Applications 2021; 29: 943-952.

Riahi Z, Priyadarshi R, Rhim J-W, Bagheri R. Gelatin-based functional films integrated with grapefruit seed extract and TiO_2 for active food packaging applications. Food Hydrocolloids 2021; 112(106314): 1-10.

Rochima E, Azhary SY, Pratama RI, Panatarani C, Joni IM. Preparation and Characterization of Nano Chitosan from Crab Shell Waste by Beads-milling Method: Preparation and characterization of nano chitosan from crab shell waste by beads-milling method. IOP Conference Series: Materials Science and Engineering 2017; 193(1): 1–6.

Rokbani H, Daigle F, Ajji A. Long- and short-term antibacterial properties of low-density polyethylene-based films coated with zinc oxide nanoparticles for potential use in food packaging. Journal of Plastic Film and Sheeting 2019; 35 (2): 117–134.

Sani MA, Maleki M, Eghbaljoo-Gharehgheshlaghi H, Khezerlou A, Mohammadian E, Liu Q, Jafari SM. Titanium dioxide nanoparticles as multifuncional surface-active materials for smart/active nanocomposite packaging films. Advances in Colloid and Interface Science 2022; 300 (2): 102593-102599.

Schaefer D, Cheung WM. Smart packaging: Opportunities and challenges. Procedia CIRP 2018; 72 (March): 1022–1027.

Shahbazi Y, Shavisi N. Chitosan Coatings Containing Mentha spicata Essential Oil and Zinc Oxide Nanoparticle for Shelf Life Extension of Rainbow Trout Fillets. Journal of Aquatic Food Product Technology 2018; 27(9): 986–997.

Shahbazi Y, Shavisi N. Characterization of active nanochitosan film containing natural preservative agents. Nanomedicine Research Journal 2018; 3 (2): 109–116.

Sharma VK, Sharma M, Usmani Z, Singh BN, Tabatabael M, Gupta VK, Tailored enzymes as next-generation food-packaging tools. Trends in Biotechnology 2022; 40(8): 1001-1017.

Somrani M, Ingles M-C, Debbabi H, Abidi F, Palop A. Garlic, Onion, and Cinnamon Essential Oil Anti-Biofilms, Effect against Listeria monocytogenes. Foods 2020; 9 (567): 1-12.

Song X, Zuo G, Chen F. Effect of essential oil and surfactant on the physical and antimicrobial properties of corn and wheat starch films Running title : Starch based films properties affected by essential oil and surfactant. International Journal of Biological Macromolecules 2017; 107(February): 1302-1309.

Spoială A, Ilie CI, Dolete G, Croitoru AM, Surdu VA, Truscă RD, Motelica L, Oprea OC, Ficai D, Ficai A, Andronescu E, Ditu LM. Preparation and Characterization of Chitosan/TiO_2 Composite Membranes as Adsorbent Materials for Water Purification. Membranes 2022; 12 (804): 1-25.

Talon E, Trifkovic KT, Nedovic VA, Bugarski BM, Vargas M, Chiralt A, González-Martĭnez C. Antioxidant edible films based on chitosan and starch containing polyphenols from thyme extracts. Carbohydrate Polymers 2017; 157 (February): 1153-1161.

Tan C, Han F, Zhang S, Li P, Shang N. Novel bio-based materials and applications in antimicrobial food packaging: Recent advances and future trends. International Journal of Molecular Sciences 2021; 22 (18): 1-19.

Varghese SA, Siengchin S, Parameswaranpillai J. Essential oils as antimicrobial agents in biopolymer-based food packaging - A comprehensive review. Food Bioscience 2020; 38: 1-89.

Wang H, Qian J, Ding F. Emerging chitosan-based films for food packaging applications. Journal of Agricultural and Food Chemistry 2017; 61 (1): 1-66.

Wang Y, Xu J, Lin W, Wang J, Yan H, Sun P. Citral and cinnamaldehyde – Pickering emulsion stabilized by zein coupled with chitosan against Aspergillus. spp and their application in food storage. Food Chemistry 2023; 403 (134272).

Winkler HC, Notter T, Meyer U, Naegeli H. Critical review of the safety assessment of titanium dioxide additives in food. Journal of Nanobiotechnology 2018; 16 (51): 1-19.

Wu H, Zhao F, Li Q, Huang J, Ju J. Antifungal mechanism of essential oil against foodborne fungi and its application in the preservation of baked food. Critical Reviews in Food Science and Nutrition 2022; 64 (9): 2695-2707.

Xing Y, Xu Q, Li X, Chen C, Ma L. Chitosan-based coating with antimicrobial agents: Preparation, property, mechanism, and application effectiveness on fruits and vegetables. International Journal of Polymer Science 2016; 1-24.

Zang W, Rhim J-W. Titanium dioxide (TiO_2) for the manufacture of multifunctional active food packaging films. Food Packaging and Shelf Life 2022; 31 (100806).